A Continuous-Flow Capillary Mixing Method to Monitor Reactions on the Microsecond Time Scale

M. C. Ramachandra Shastry,* Stanley D. Luck,* and Heinrich Roder*#

*Institute for Cancer Research, Fox Chase Cancer Center, Philadelphia, Pennsylvania 19111, and #Department of Biochemistry and Biophysics, University of Pennsylvania, Philadelphia, Pennsylvania 19104-6059 USA

ABSTRACT A continuous-flow capillary mixing apparatus, based on the original design of Regenfuss et al. (Regenfuss, P., R. M. Clegg, M. J. Fulwyler, F. J. Barrantes, and T. M. Jovin. 1985. *Rev. Sci. Instrum.* 56:283–290), has been developed with significant advances in mixer design, detection method and data analysis. To overcome the problems associated with the free-flowing jet used for observation in the original design (instability, optical artifacts due to scattering, poor definition of the geometry), the solution emerging from the capillary is injected directly into a flow-cell joined to the tip of the outer capillary via a ground-glass joint. The reaction kinetics are followed by measuring fluorescence versus distance downstream from the mixer, using an Hg(Xe) arc lamp for excitation and a digital camera with a UV-sensitized CCD detector for detection. Test reactions involving fluorescent dyes indicate that mixing is completed within 15 μs of its initiation and that the dead time of the measurement is 45 $\pm$ 5 μs, which represents a >30-fold improvement in time resolution over conventional stopped-flow instruments. The high sensitivity and linearity of the CCD camera have been instrumental in obtaining artifact-free kinetic data over the time window from ~45 μs to a few milliseconds with signal-to-noise levels comparable to those of conventional methods. The scope of the method is discussed and illustrated with an example of a protein folding reaction.

INTRODUCTION

Rapid mixing of two or more solutions is the most versatile and generally applicable method of initiating chemical reactions and biological processes. Methods like stopped flow and quenched flow coupled with optical detection, NMR, or electron paramagnetic resonance have been especially important for elucidating mechanisms of enzyme catalysis and protein folding (Fersht, 1985; Roder, 1989; Kuwajima et al., 1989; Kim and Baldwin, 1990; Matthews, 1993). The time resolution of a fast mixing device is determined by the instrumental dead time, which depends critically on the time required to achieve complete mixing of the two reagents (mixing time), the flow velocity, and the volume between the mixing region and the point of observation (dead volume). Although it is difficult to precisely measure the mixing time and dead volume, the dead time is operationally well defined in terms of the observable amplitude of simple first-order reactions (Tonomura et al., 1978; Paul et al., 1980; Brissette et al., 1989). Rapid mixing experiments involving optical detection can be broadly divided into continuous-flow (CF) and stopped-flow (SF) methods (Hartridge and Roughton, 1923; Chance, 1940; Gibson and Milnes, 1964). The latter is more commonly used because of its sample economy and the ability to measure the kinetics out to long times (typically minutes, limited by diffusion and convection artifacts). However, the time window accessible to SF is generally limited to 2 ms or longer, as measurements are made only after the flow comes to a complete stop, which is inherently slow and can result in vibration and pressure artifacts. Somewhat shorter dead times can be achieved by using the CF methodology, in which two (or more) solutions pumped at high linear velocities through different channels are brought into contact in a small mixing volume, and complete mixing can be achieved within fractions of a millisecond (Kletenik, 1963). The progress of the reaction is followed downstream from the mixer along the flow direction, which is translated into time on the basis of the known flow rate and dimensions of the flow channel. An especially elegant method was introduced by Regenfuss et al. (1985), who developed a capillary mixer by combining the idea of concentric glass capillaries (Moskowitz and Bowman, 1966) with aspects of the Berger-type ball mixer (Berger et al., 1968a). However, there have been few practical applications of this mixer design, because of the difficulty of manufacturing such devices and the inefficient detection method.

The fundamental process that leads to complete mixing of two solutions at the molecular level is diffusion. An ideal mixer would completely intersperse the reactants before the reaction can progress to a considerable extent. Turbulence provides an efficient mechanism for rapid mixing by dispersing the solutions into small volume elements (turbulent eddies); mixing is rapid and efficient because diffusion now has to occur over very short distances. Berger et al. (1968a,b) recognized that this can be achieved by pumping two solutions with high velocity around a sphere. Thus the key for designing an efficient mixer is to obtain high flow velocities in the mixing region so as to make linear dimensions of the turbulent eddies as small as possible while

Received for publication 8 January 1998 and in final form 20 January 1998.

Address reprint requests to Dr. Heinrich Roder, Institute for Cancer Research, Fox Chase Cancer Center, 7701 Burholme Ave., Philadelphia, PA 19111. Tel.: 215-728-3123; Fax: 215-728-3574; E-mail: H Roder@fccc.edu.

Dr. Luck's present address is E. I. du Pont de Nemours and Co., Experimental Station, Wilmington, DE 19880.

0006-3495/98/05/2714/08 $2.00

confining the region required for complete mixing to a minimum.

Based on these criteria, Regenfuss et al. (1985) designed a simple capillary jet mixing device consisting of two coaxial glass capillaries with a small platinum sphere positioned at the tip of the inner capillary, such that highly turbulent flow conditions are generated in a ~10-μm gap between the sphere and the outer capillary. The solution emerged as a thin jet at a high linear velocity, and the progress of the reaction was followed by measuring fluorescence emission versus distance downstream from the mixer. By observing the binding of a fluorescent dye, 1-anilino-8-naphthalene-sulfonic acid (ANS), to the protein bovine serum albumin (BSA), they were able to resolve a reaction with a time constant of ~100 μs with an effective dead time of 60–80 μs. Despite these impressive results, there has been only one subsequent paper reporting minor modifications to their design in conjunction with Raman scattering measurements (Paeng et al., 1994). Takahashi et al. (1997) recently reported CF resonance Raman studies of heme ligation and folding of cytochrome *c* (cyt *c*), using a machined T-mixer with a dead time of 100 ± 50 μs, and Chan et al. (1997) combined a similar mixer with a UV laser source and a diode array to follow tryptophan fluorescence changes during folding.

In their jet mixing experiment, Regenfuss et al. (1985) used a conventional camera for fluorescence detection. However, standard high-speed monochrome film is inadequate for this application, because of its low sensitivity in the UV region, limited dynamic range, and nonlinear light response. Moreover, processing and image analysis are cumbersome and time-consuming. The laser resonance Raman method used for detection in several studies of enzyme and protein folding reactions (Paeng et al., 1994; Takahashi et al., 1995, 1997) is limited to certain systems with a suitable chromophore, such as a heme group. We have been able to overcome these limitations by incorporating a digital camera with a UV-coated charge-coupled device (CCD) detector into our instrument.

INSTRUMENT DESIGN AND CONSTRUCTION

The mixer

In contrast to earlier mixers, which were made of glass (Moskowitz and Bowman, 1966; Regenfuss et al., 1985), we used quartz tubing and rods to construct our capillary mixer, which offers higher mechanical stability and superior optical properties in the UV region. The inner capillary is prepared by manual pulling of the heated quartz tubing (3 mm o.d., 1 mm i.d.). For the outer capillary, wider tubing (6 mm o.d., 4 mm i.d) is first constricted and then pulled with the aid of a glass blowing lathe. A platinum wire (50 μm diameter; Good Fellow, Berwyn, PA) is passed through the inner capillary (~250-μm-diameter opening), and a spherical bead is formed at its tip by melting the end in a small flame. The inner capillary along with the bead is positioned carefully inside the tapered end of the outer capillary. Thin glass rods (10 μm diameter), fused to the inner wall of the outer capillary, prevent the platinum bead from plugging the outlet. The inner and outer capillaries are held together by nylon reducing union (1/8–1/4″; Penn Valve and Fitting Co., Willow Grove, PA).

CF instruments involving a free-flowing jet encounter severe problems due to the instability and poor definition of the jet and scattering artifacts. To overcome these problems, we incorporated a fluorescence flow cell with a path length of 0.25 mm (Hellma Cells, Jamaica, NY) into our design. The solution emerging from the mixer is directly injected into the 0.25 mm × 0.25 mm channel of the observation cell. A challenging engineering problem was to achieve a tight connection between the mixer and the flow cell that could withstand pressures of up to 10 atmospheres while minimizing the dead volume. We have found that a ground-glass joint offers the best solution. The mixer is mounted on top of the observation cell placed in a thermostatted brass sample holder. The temperature of the solution was measured with a thermocouple (0.02-inch diameter, KMTSS-020-G-6; Omega Engineering, Stratford, CT) placed at the exit of the flow cell.

Sample delivery and detection

A diagram of the experimental arrangement is shown in Fig. 1. Pneumatically driven syringes deliver the reactants to be studied into each of the two coaxial capillaries. The teflon tubing carrying the solution to the capillaries is fitted with in-line Ti filters (0.2-μm pore size; Varian Corporation, Palo Alto, CA). The solution to the outer capillary is injected via a hypodermic needle fitted through the sides of the plastic reducing union. The reagents are forced through the narrow gaps between the sphere and the outer capillary, where mixing occurs under highly turbulent flow conditions. The completely mixed solution emerging from the mixer is injected into the 0.25 mm × 0.25 mm flow channel of the fused quartz observation cell. The progress of a reaction is followed by recording the fluorescence profile versus distance along the flow channel. A conventional light source consisting of a 150-W Xe/Hg arc lamp (L-2482; Hamamatsu, Japan), collimating optics, and a monochromator is used for fluorescence excitation. Relatively uniform illumination of the flow channel over a length of 5–10 mm is achieved with the help of a cylindrical lens (Oriel Corporation, Stratford, CT). A complete fluorescence versus distance profile is obtained by imaging the fluorescent light emitted at a 90° angle onto a digital camera system (type RTE/CCD-1317-K, MicroMax; Princeton Instruments, Princeton, NJ) containing a UV-coated CCD chip with an array of 1317 × 1035 pixels (Kodak KAF-1400). The camera is equipped with a fused silica magnifying lens (28-mm focal length, 25-mm diameter) and a high-pass glass filter or a band-pass interference filter to suppress scattered incident light (both from Oriel Corporation). The

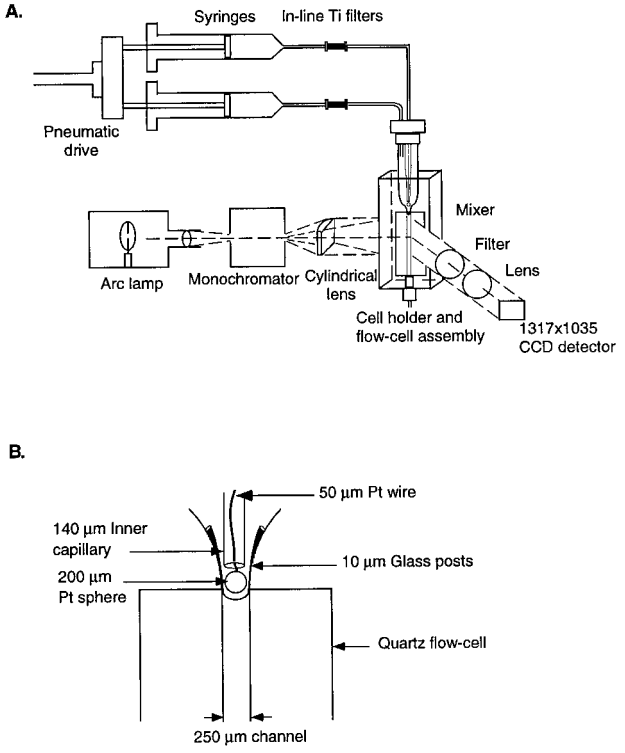

FIGURE 1 Schematic diagram of the capillary mixing apparatus. (*A*) Overview of the experimental arrangement, including solution delivery, the mixer assembly, flow cell, light source, optical components, and detector. (*B*) The mixing region near the tip of the outer capillary and the observation cell are shown expanded for clarity.

total flow rate of the solution was determined by weighing water passed through both of the capillaries at a given pressure and for a known period of time. Typical flow rates of 0.6 ml/s are obtained at a pressure of 5 atm, which results in a linear velocity of ~10 m/s through the channel of the observation cell. There is no evidence of turbulence extending into the channel (see Operation and Performance), and the flow appears to be laminar. By changing the magnification of the camera and the flow rate of the solution, the observable time starting from ~45 μs (the shortest dead time achieved so far; see below) to an upper limit of ~2 ms can be achieved, joining the time scale accessible to conventional SF measurements (see below).

OPERATION AND PERFORMANCE

Data collection and analysis

The most important new feature of our apparatus is the utilization of a CCD camera as a detector. The UV-sensitized Kodak chip used in the camera offers excellent sensitivity and resolution over the spectral range of interest to most biological applications (200–1000 nm). Data are collected in digital form by acquiring as many as 1317 points simultaneously and are displayed in seconds. Processing of these images with standard image analysis software takes no more than a few minutes. The sensitivity of detection and efficiency of data collection are essential for routine analysis, especially for biological applications. In contrast, the use of lasers in some previous studies (Paeng et al., 1994; Takahashi et al., 1995, 1997) to measure the signal (Raman scattering or fluorescence) at a single time point along the flow direction requires dozens of separate experiments to generate a complete time course at a much higher cost, in both time and materials.

A representative example of a kinetic experiment is illustrated in Fig. 2. The reaction was followed by recording an image during continuous-flow mixing of a fluorophore, *N*-acetyltryptophanamide (NATA), with the chemical quencher *N*-bromosuccinimide (NBS) at final concentrations of 40 μM and 8 mM, respectively. Fig. 2 *A* shows a profile of the emitted light intensity versus distance along the flow channel measured with the image analysis software (*WinView*, version 1.6.1.) supplied with the digital camera. Intensity profiles are obtained by averaging a series of cross

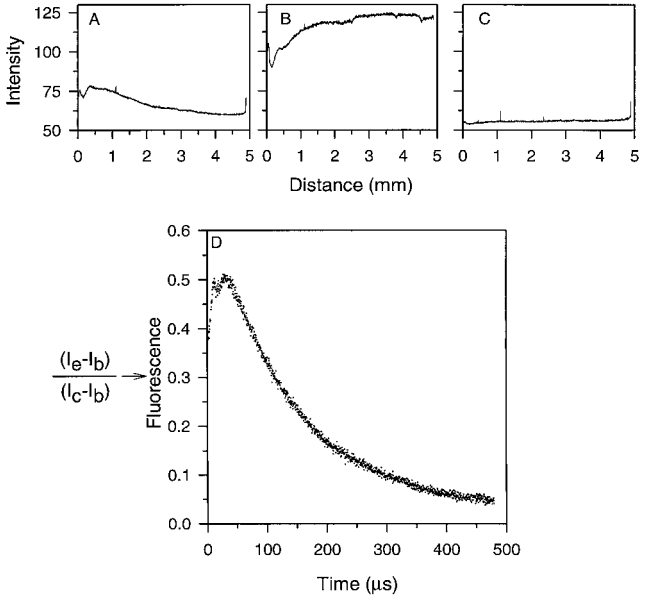

FIGURE 2 A typical continuous-flow mixing experiment, illustrating data acquisition and analysis. Solutions of NATA and NBS were prepared in 20 mM phosphate (pH 7). Syringes and the sample holder were thermostatted at 24°C. In *A*, *B*, and *C* the tip of the capillary mixer coincides with the origin of the *x* axis, which represents distance from the mixing region along the flow channel. (*A*) Intensity profile obtained for the quenching reaction of NATA by NBS (I_e); the final concentrations of NATA and NBS were 40 μM and 8 mM, respectively. (*B*) Intensity profile of the unquenched fluorescence control (I_c); fluorescent NATA solution (40 μM) was mixed with buffer alone to account for variations in light intensity along the flow channel. (*C*) Intensity profile of the background control (I_b); buffer alone was passed through both of the capillaries to account for any scattering artifacts and to record the background intensity from the CCD camera. (*D*) Corrected kinetic fluorescence trace, calculated according to Eq. 1, using the intensities I_e, I_c, and I_b from profiles *A*, *B*, and *C*, respectively. The origin of the axis is arbitrary, but corresponds approximately to the point at which mixing is completed, just below the platinum sphere. While fitting the data (Fig. 3), time points corresponding to the first 45 μs (dead time) are not included, as they correspond to the intensity obtained from within the mixer.

sections (at a resolution of one pixel) along the flow direction so as to cover the entire width of the flow channel. Approximately 30 individual cross sections make up each intensity profile. To account for spatial variations in the incident light intensity, a control experiment was performed in which the same NATA solution was mixed with buffer in the absence of NBS (Fig. 2 *B*). A second control experiment on buffer solutions (or water) under identical flow conditions (Fig. 2 *C*) accounts for any background signal due to scattered or reflected incident light passing through the filter and the background level of the CCD detector. Fig. 2 *D* shows a plot of the corrected relative fluorescence (fl_{rel}) versus time, calculated according to

$$fl_{rel} = (I_e - I_b)/(I_c - I_b) \quad (1)$$

where I_e, I_c, and I_b are the raw intensities from experiment, control, and background measurements, respectively. This procedure accounts for any variable excitation along the flow channel and background contributions, yielding fluorescence relative to a well-defined reference. The time axis was calibrated on the basis of the measured flow rate, the known dimensions of the flow cell, and magnification of the camera lens. The fluorescence decay is accurately described by a single-exponential function with a time constant of 185 ± 15 μs. In this representative example, a signal-to-noise (S/N) ratio of 70:1 was obtained in an 8-s exposure in both experiment and control, consuming a total of 10 ml of a 40 μM NATA (tryptophan) solution. Total experiment time, including data analysis, was ~10 min.

Mixing efficiency

To determine the mixing efficiency of the apparatus, intensity profiles from two experiments were compared. In the first experiment, a solution of NATA was diluted 11-fold, and a fluorescence profile was recorded under continuous-flow conditions. In the second experiment, the same NATA stock solution diluted 11-fold outside of the mixer was delivered through both of the capillaries, and the intensity profile was again recorded under identical flow conditions. The ratio of the two profiles after appropriate background correction was very close to unity, suggesting that the fluorescent solution was completely mixed before it entered the observation cell (data not shown).

To account for any mixing artifacts, such as turbulence entering the observation cell or cavitation effects, the intensity profiles of the premixed fluorescent solution were compared during continuous flow (0.62 ml/s) and under static conditions. There was no indication of any difference between the two profiles, and the ratio of the intensities was again close to unity.

The same two performance tests have been repeated at different flow rates. At flow rates lower than 0.35 ml/s, intensity profiles orthogonal to the flow direction become nonuniform, and the intensity ratio is less than unity in the beginning and approaches unity only further downstream, indicating that the solutions were not completely mixed before entering the observation cell. When flow rates higher than 0.9 ml/s were employed, erratic scattering artifacts appeared near the entrance to the flow channel, which would not cancel out in the final fluorescence trace, indicating that turbulence or cavitation artifacts had extended into the observation cell. In experiments with proteins (cyt *c*, staphylococcal nuclease, and BSA), we found no evidence for degradation or fragmentation, based on sodium dodecyl sulfate gel electrophoresis of the protein before and after passing through the mixer. Considering the moderate pressure utilized in these experiments, any reversible distortion of the polypeptide due to shear forces is also likely to be minimal. This was confirmed by measurements on acid-unfolded cyt *c* at different flow rates, which showed no flow-induced changes in tryptophan-heme fluorescence energy transfer (a sensitive measure of overall chain dimensions).

Dead time

A method routinely used to determine the dead time of a rapid mixing device is to observe the fluorescence decay of the tryptophan analog NATA induced by its reaction with NBS (Peterman, 1979). The pseudo-first-order quenching reaction of NATA by NBS was measured at NBS concentrations from 2 to 32 mM, where the reaction exhibits time constants ranging from 300 to 40 μs. Shown in Fig. 3 is a semilogarithmic plot of the corrected fluorescence traces obtained at different NBS concentrations. The solid lines represent single-exponential fits obtained by nonlinear regression. All of the data extrapolate to a common point near $fl_{rel} = 1$, the expected initial fluorescence (that of NATA in the absence of quencher). The time delay from this point to the first data point that falls on the fitted exponential provides an estimate of the dead time (45 ± 5 μs) of the measurement.

Accuracy

Fig. 3 *B* shows a linear plot of the measured rates as a function of NBS concentration. The second-order rate constant obtained (7.9×10^5 M^{-1} s^{-1}) is in excellent agreement with published results (Peterman, 1979) measured at much lower NBS concentration (7.3×10^5 M^{-1} s^{-1}), confirming the accuracy and reliability in measuring the rate constants as fast as 2.5×10^4 s^{-1}. The low noise level and high quality of the kinetic data make it possible to measure time constants that are shorter than the dead time of the apparatus.

The same experiment was also carried out with NATA in the presence of 4.5 M GdnHCl (to mimic the conditions of a typical protein folding experiment). The dead time obtained (48 ± 3 μs) was within error of that in the absence of denaturant, excluding any flow artifacts due to the difference in densities and viscosities of the two liquids flowing through the two capillaries.

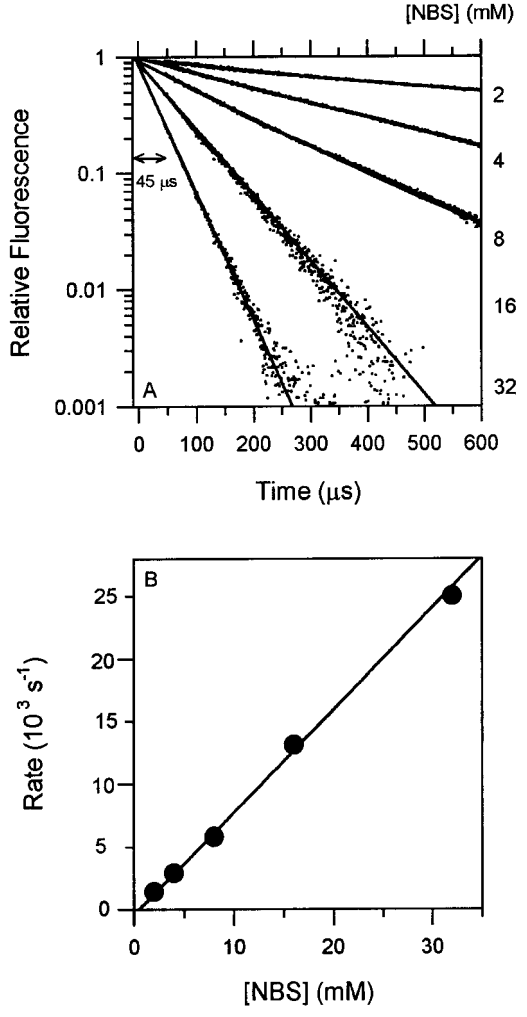

FIGURE 3 Dead-time calibration and accuracy of measurements of the capillary mixer. (*A*) A plot of the fluorescence quenching reaction of NATA by NBS as a function of [NBS]. Experimental conditions are as in Fig. 2. Solid lines are single exponential fits to the data. The point of concurrence of all the traces corresponds to the time of complete mixing, 45 ± 5 μs before the first observable data point. (*B*) First-order reaction rate constants of quenching of NATA by NBS versus [NBS]. The solid line through the data points is the linear fit, yielding a second-order rate constant of 7.9×10^5 M^{-1} s^{-1}, which agrees very well with the literature value of 7.3×10^5 M^{-1} s^{-1} (Peterman, 1979).

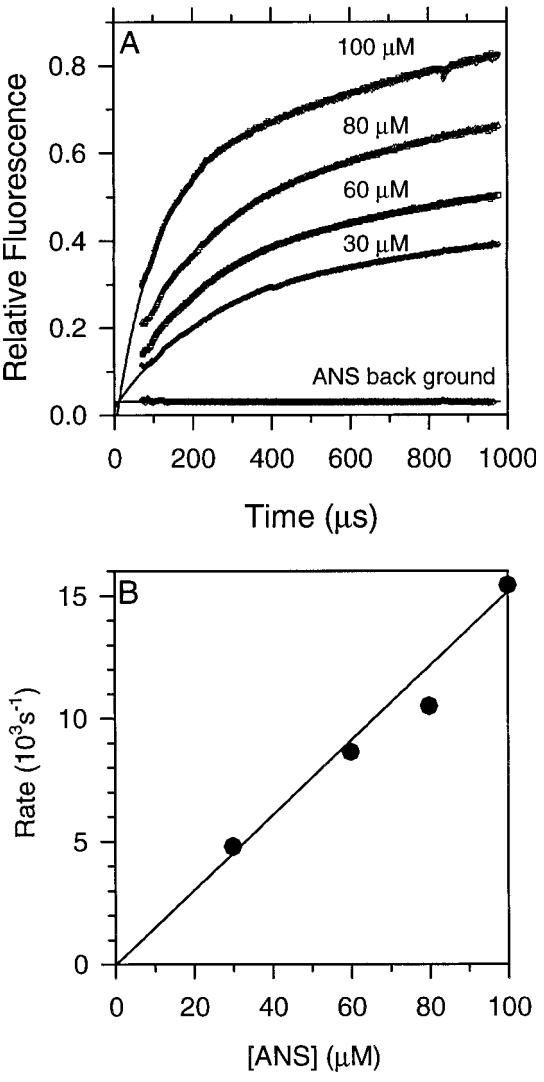

FIGURE 4 Kinetics of ANS binding to BSA at 24°C. The solutions of ANS and BSA were prepared in 100 mM phosphate (pH 7). ANS fluorescence was excited at 366 nm, and fluorescence emission was recorded above 418 nm. (*A*) Series of CF kinetic traces representing the increase in ANS fluorescence due to binding to BSA. Solid lines through the curves are the double-exponential fits to the data with time constants of 220 μs and 2 ms (30 μM) and 66 μs and 2.8 ms (100 μM). (*B*) Measured rate constants of the faster phase plotted as a function of concentration of ANS. The solid line is a linear fit to the data points. The corresponding second-order reaction rate constant, 3.5×10^8 M^{-1} s^{-1}, is in good agreement with the value reported in the literature (Gibson and Antonini, 1966).

Gibson and Antonini (1966) studied the binding of the hydrophobic dye ANS to the model protein BSA by the conventional SF method and derived an apparent association rate constant of ANS to BSA sites of $\sim 5.0 \times 10^8$ M^{-1} s^{-1}. We measured the increase in the fluorescence at 450 nm associated with the binding of ANS to BSA under similar conditions, but with much higher concentrations of ANS than previously employed. Fig. 4 *A* shows a series of kinetic traces at different ANS concentrations (30–100 μM). Double-exponential curves provide excellent fits to all of the data, as exemplified by the solid lines through the data at ANS concentrations of 30 μM and 100 μM. The time constant of the faster phase ranges between 200 μs (at 30 μM ANS) and 70 μs (at 100 μM ANS). The observed rate constants show a linear increase, within error, with ANS concentration reaching a rate of 1.5×10^4 s^{-1} at 100 μM (Fig. 4 *B*). The corresponding second-order rate constant (3.5×10^8 M^{-1} s^{-1}) agrees well with the published value (Gibson and Antonini, 1966), again demonstrating the reliability of the measurements.

Estimated mixing time

Although optical distortions and light reflections preclude reliable quantitative measurements inside the tip of the

capillary mixer, the test measurements shown in Figs. 3 and 4 clearly indicate that the time required to achieve complete mixing of the two reagents must be much shorter than the instrumental dead time (45 μs); if this were not the case, the traces would not extrapolate to a common point and would deviate from the exponential behavior at early times. A rough estimate of the mixing time of the instrument can be obtained as follows. Inspection of the images in the mixing region shows that the fluorescent solution passed through the inner capillary forms a cylindrical stream (with a diameter approximately equal to that of the platinum sphere, 250 μm) and does not enter significantly into the regions of the outer capillary above the sphere. Thus it is reasonable to assume that the flow rate is approximately constant below the platinum bead. With the present mixer, the first reliable data start from a point ~600 μm downstream from the bottom of the sphere. At a linear velocity of 10 m/s, this distance translates into a travel time of ~60 μs. This means that the first reliable data start 60 μs after the initiation of the mixing process. Because the measured dead time was ~45 μs, this suggests that mixing must be completed within ~15 μs after initiation. The region within which mixing is completed extends ~150 μm below the bead. Assuming a cylindrical geometry for the stream of the solution, this corresponds to an estimated mixing volume of ~8 pl and a dead volume of the instrument of ~30 pl.

Comparison of CF and SF methods

The test results and the experiments described here demonstrate that our CF capillary mixing method makes it possible to probe reactions down to the 40-μs range, which represents an improvement of at least 30-fold in time resolution over commercially available SF instruments, which achieve a dead time of ~1.5 ms at best. At the same time, the kinetic fluorescence measurements are highly reproducible, and the quality of the kinetic data is comparable to that obtained with conventional SF methods. Unlike stopped flow, the CF approach does not suffer from artifacts due to pressure, vibration, or cavitation (although they can surface at high flow rates). CF measurements are not fraught with artifacts due to convection, optical bleaching of the chromophore, or fluctuations in light intensity that often limit the quality of SF data. The high sensitivity of the CCD detector makes it possible to work with relatively small amounts of reagents. For example, in a typical CF experiment consuming 4×10^{-7} moles of the protein cyt *c*, we obtained a S/N ratio of 70:1, whereas an identical experiment on an SF instrument (Bio-Logic SFM-4 with MOS-200 optics; Bio-Logic, Claix, France) required 1×10^{-7} moles of cyt *c* and resulted in a S/N ratio of 130:1. Moreover, contamination from the reacted solution from the previous mixing event is of lesser concern in CF experiments because of the large volumes injected. However, temperature change due to an endothermic or exothermic reaction is a problem with both methods. The main limitation of the CF method at this stage is the difficulty in acquiring data beyond ~3 ms. Thus it is still necessary to perform SF experiments under identical conditions to complement the CF data.

APPLICATION TO PROTEIN FOLDING

A major advantage of the capillary mixer described in this paper is that it can be used to study any fast reaction involving the mixing of two solutions producing a change in fluorescence (the possibility of absorbance or circular dichroism will be explored in future work). One of the unsolved problems in biochemistry is understanding the mechanism of protein folding, the process by which an unstructured chain of amino acids navigates itself to find the most stable three-dimensional structure amid countless possible pathways. In many proteins, major conformational changes are known to take place during early stages of folding (Matthews, 1993; Roder and Elöve, 1994; Ptitsyn, 1995; Miranker and Dobson, 1996; Roder and Colón, 1997). These submilliseond processes were largely inaccessible until recently, although their existence was implied by the observation of "missing amplitude" in SF experiments (Kuwajima et al., 1987; Elöve et al., 1992; Parker et al., 1995; Khorasanizadeh et al., 1996; Sauder et al., 1996; Park et al., 1997). The capillary mixer offers a unique way of monitoring reactions on the submillisecond time scale from a time point as early as 40 μs.

The fluorescence of the sole tryptophan (Trp^{59}) in horse cyt *c* is quenched efficiently upon folding via energy transfer to the covalently bound heme. Thus fluorescence provides a convenient qualitative measure of compactness in terms of the average distance between Trp^{59} and the heme. This property has been exploited in earlier studies on the folding mechanism of cyt *c* (Tsong, 1976; Brems and Stellwagen, 1983; Roder et al., 1988; Elöve et al., 1992, 1994; Jones et al., 1993; Colón et al., 1996). Previous SF experiments demonstrated that under stable refolding conditions, a significant fraction of the expected total fluorescence change occurs during the ~2-ms dead time of the apparatus, indicating rapid formation of a compact intermediate (Elöve et al., 1992; Colón et al., 1996). Kinetic CD measurements showed that this intermediate contains native-like helical secondary structure (Elöve et al., 1992). As the collapse event was never directly observed, it has been unclear whether these submillisecond processes reflect a diffusion-controlled nonspecific collapse of the chain (Sosnick et al., 1994, 1996; Chan et al., 1997), or whether they represent formation of a more specifically organized structural intermediate (Colón et al., 1996; Sauder and Roder, manuscript submitted for publication).

Using the capillary mixer, we were able to directly observe the previously unresolved submillisecond kinetics during folding of cyt *c*. A solution of unfolded cyt *c* at pH 2 and 22°C was diluted with buffer (50 mM sodium acetate, 50 mM sodium phosphate) to a final pH value of 4.5. As a fluorescence control (I_c in Eq. 1), the same unfolded solu-

tion at pH 2 was mixed with 10 mM HCl, conditions in which the protein remains in its fluorescent unfolded state. A representative kinetic trace is shown in Fig. 5 *A*. The observed fluorescence decay has been fitted to a biexponential function consisting of a major fast phase with a time constant of 57 ± 6 μs (60% of the amplitude), and a slower phase with a time constant of 454 ± 19 μs (20% of the amplitude). The observation that the fitted curve extrapolates to a relative fluorescence of unity indicates that our measurements on the submilliseond time scale quantitatively account for the complete fluorescence change associated with refolding of cyt *c*. The low fluorescence level reached after the fast phase (~60% of the unfolded reference sample at pH 2) is indicative of a well-populated intermediate with significantly quenched fluorescence corresponding to a short average tryptophan-heme distance. The fact that the initial fluorescence decay is exponential indicates that there is a well-defined kinetic barrier separating this compact state from unfolded conformations. A detailed account of the kinetics of cyt *c* folding as a function of pH and GdnHCl will appear elsewhere (Shastry and Roder, manuscript submitted for publication).

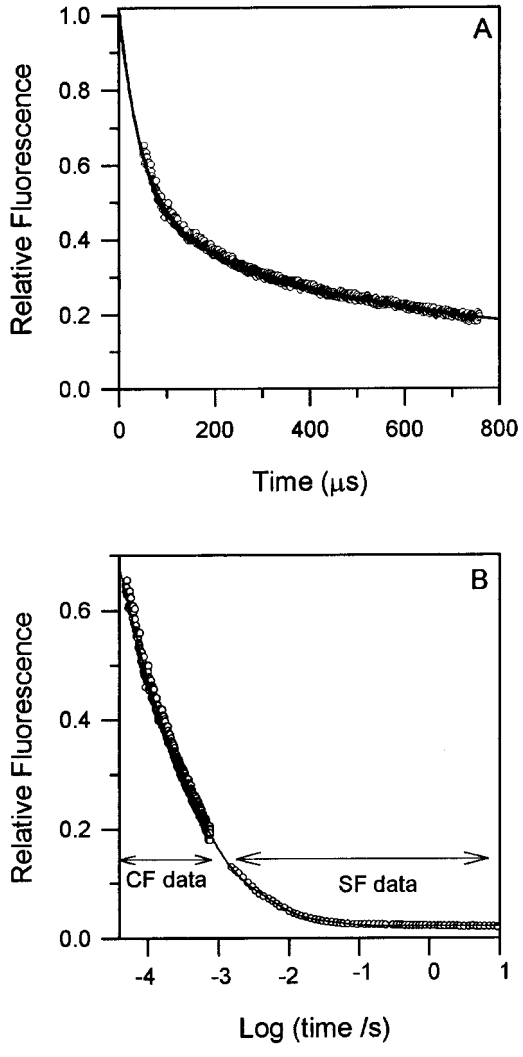

FIGURE 5 Submillisecond folding kinetics of cytochrome *c*. Acid-unfolded horse cytochrome *c* (40 μM) in 10 mM HCl (pH 2) was mixed with buffer of higher pH, to obtain a final pH of 4.5 at 22°C (conditions favoring rapid formation of the native structure). Horse heart cytochrome *c* (highest grade from Sigma Chemical Co., St. Louis, MO) has been desalted on a Sephadex G-25 column, equilibrated with 10 mM HCl. The solutions were filtered through a 0.2-μm-pore filter and degassed before use. Tryptophan fluorescence was excited at 280 nm, and fluorescence emission was detected above 324 nm; excitation and emission slit widths of the monochromator were both set to 2 mm. (*A*) Submillisecond kinetics measured on the CF capillary mixing apparatus plotted on a linear time scale. The solid line represents the double-exponential fit with time constants of 57 μs and 454 μs. (*B*) Combined plot of the data obtained by capillary mixing and SF mixing experiments under identical conditions. A minimum of five exponentials have to be used to fit the combined curve by nonlinear least-squares regression. The time constants (τ) and amplitudes (a) of different kinetic phases are $\tau_1 = 57$ μs, $a_1 = 0.61$; $\tau_2 = 454$ μs, $a_2 = 0.29$; $\tau_3 = 700$ μs, $a_3 = 0.08$; $\tau_4 = 5.1$ ms, $a_4 = 0.03$; $\tau_5 = 43$ ms, $a_5 = 0.03$.

To extend the kinetics of folding to longer times, we have also monitored the reaction shown in Fig. 5 *A* on a SF instrument with a dead time of ~2 ms under identical experimental conditions. These data have been normalized independently with respect to the unfolded signal of the protein in pH 2 buffer in the respective experiments, but are analyzed together and are plotted in Fig. 5 *B* on a log time scale. The combined data have been fitted to five exponentials (Shastry and Roder, manuscript submitted for publication). Under the stabilizing folding condition chosen, only ~15% of the total fluorescence change is observed with SF measurements, whereas the CF data resolve an additional 50% of the total signal associated with the refolding between 45 μs and 1 ms. To our knowledge, this is the first report of a folding reaction monitored over about six decades of time between tens of microseconds and minutes.

SUMMARY

Novel features of the continuous-flow capillary mixing method described here include 1) use of quartz to construct a mixer with improved characteristics; 2) joining the tip of the outer capillary to the flow cell through a ground-glass joint, resulting in minimal dead volume; 3) the use of a CCD camera to replace the conventional camera for detection. The instrumental dead time of 45 μs achieved is shorter than that of any mixing apparatus reported to date. Its application to the problem of protein folding has conclusively demonstrated that the early steps in the folding of cyt *c* are conformational events separated by distinct energy barriers (Shastry and Roder, manuscript submitted for publication). Straightforward modifications of the flow cell and optical arrangement should make it possible to adapt the method to absorbance or CD measurements as well. Possible applications, in addition to the examples described here, include studies of chemical and enzymatic reaction mechanisms, ligand binding, as well as numerous other rapid processes of biological interest.

We thank G. D. Markham, S-H. Park, and J. Murphy for their comments on the manuscript and John Moeller for his help in construction of the sample holder.

This work was supported by National Science Foundation grant MCB-9306367, National Institutes of Health grants GM35926 (to HR) and CA06927, and an appropriation from the Commonwealth of Pennsylvania to the Institute for Cancer Research. MCRS was supported by a fellowship from the Board of Associates of the Fox Chase Cancer Center.

REFERENCES

Berger, R. L., B. Balko, W. Borcherdt, and W. Friauf. 1968b. High speed optical stopped-flow apparatus. *Rev. Sci. Instrum.* 39:486–493.

Berger, R. L., B. Balko, and H. F. Chapman. 1968a. High resolution mixer for the study of the kinetics of rapid reactions in solution. *Rev. Sci. Instrum.* 39:493–498.

Brems, D. N., and E. Stellwagen. 1983. Manipulation of the observed kinetic phases in the refolding of denatured ferricytochromes c. *J. Biol. Chem.* 258:3655–3660.

Brissette, P., D. P. Ballou, and V. Massey. 1989. Determination of the dead time of a stopped-flow fluorometer. *Anal. Biochem.* 181:234–238.

Chan, C.-K., Y. Hu, S. Takahashi, D. L. Rousseau, W. A. Eaton, and J. Hofrichter. 1997. Submillisecond protein folding kinetics studied by ultrarapid mixing. *Proc. Natl. Acad. Sci. USA.* 94:1779–1784.

Chance, B. 1940. The accelerated-flow method for rapid reactions. I. *Anal. J. Franklin Inst.* 229:455–613.

Colón, W., G. A. Elöve, L. P. Wakem, F. Sherman, and H. Roder. 1996. Side chain packing of the N- and C-terminal helices plays a critical role in the kinetics of cytochrome c folding. *Biochemistry.* 35:5538–5549.

Elöve, G. A., A. K. Bhuyan, and H. Roder. 1994. Kinetic mechanism of cytochrome c folding: involvement of the heme and its ligands. *Biochemistry.* 33:6925–6935.

Elöve, G. A., A. F. Chaffotte, H. Roder, and M. E. Goldberg. 1992. Early steps in cytochrome c folding probed by time-resolved circular dichroism and fluorescence spectroscopy. *Biochemistry.* 31:6876–6883.

Fersht, A. 1985. Enzyme Structure and Mechanism. W. H. Freeman and Company, New York.

Gibson, Q. H., and E. Antonini. 1966. kinetics of heme-protein intractions. *In* Hemes and Hemeproteins. Academic Press, New York. 67–78.

Gibson, Q. H., and L. Milnes. 1964. *Biochem. J.* 91:161.

Hartridge, H., and F. J. W. Roughton. 1923. Method of measuring the velocity of very rapid chemical reactions. *Proc. R. Soc. Lond. A Math. Phys. Sci.* 104:376–394.

Jones, C. M., E. R. Henry, Y. Hu, C.-K. Chan, S. D. Luck, A. Bhuyan, H. Roder, J. Hofrichter, and W. A. Eaton. 1993. Fast events in protein folding initiated by nanosecond laser photolysis. *Proc. Natl. Acad. Sci. USA.* 90:11860–11864.

Khorasanizadeh, S., I. D. Peters, and H. Roder. 1996. Evidence for a three-state model of protein folding from kinetic analysis of ubiquitin variants with altered core residues. *Nature Struct. Biol.* 3:193–205.

Kim, P. S., and R. L. Baldwin. 1990. Intermediates in the folding reactions of small proteins. *Annu. Rev. Biochem.* 59:631–660.

Kletenik, Y. B. 1963. A mixer for investigating the kinetics of rapid reactions in solutions by the flow method. *J. Phys. Chem. USSR.* 37:638–640.

Kuwajima, K., M. Mitani, and S. Sugai. 1989. Characterization of the critical state in protein folding. Effects of guanidine hydrochloride and specific Ca^{2+} binding on the folding kinetics of α-lactalbumin. *J. Mol. Biol.* 206:547–561.

Kuwajima, K., H. Yamaya, S. Miwa, S. Sugai, and T. Nagamura. 1987. Rapid formation of secondary structure framework in protein folding studied by stopped-flow circular dichroism. *FEBS Lett.* 221:115–118.

Matthews, C. R. 1993. Pathways of protein folding. *Annu. Rev. Biochem.* 62:653–683.

Miranker, A. D., and C. M. Dobson. 1996. Collapse and cooperativity in protein folding. *Curr. Opin. Struct. Biol.* 6:31–42.

Moskowitz, G. W., and R. L. Bowman. 1966. A multicapillary mixer of solutions. *Science.* 153:428–429.

Paeng, K., I. Paeng, and J. Kincaid. 1994. Time-resolved resonance Raman spectroscopy using a fast mixing device. *Anal. Sci.* 10:157–159.

Park, S.-H., K. T. O'Neil, and H. Roder. 1997. An early intermediate in the folding reaction of the B1 domain of protein G contains a native-like core. *Biochemistry.* 36:14277–14283.

Parker, M. J., J. Spencer, and A. R. Clarke. 1995. An integrated kinetic analysis of intermediates and transition states in protein folding reactions. *J. Mol. Biol.* 253:771–786.

Paul, C., K. Kirschner, and G. Haenisch. 1980. Calibration of stopped-flow spectrophotometers using a two-step disulfide exchange reaction. *Anal. Biochem.* 101:442–448.

Peterman, B. F. 1979. Measurement of the dead time of a fluorescence stopped-flow instrument. *Anal. Biochem.* 93:442–444.

Ptitsyn, O. B. 1995. Structures of folding intermediates. *Curr. Opin. Struct. Biol.* 5:74–78.

Regenfuss, P., R. M. Clegg, M. J. Fulwyler, F. J. Barrantes, and T. M. Jovin. 1985. Mixing liquids in microseconds. *Rev. Sci. Instrum.* 56: 283–290.

Roder, H. 1989. Structural characterization of protein folding intermediates by proton magnetic resonance and hydrogen exchange. *Methods Enzymol.* 176:446–473.

Roder, H., and W. Colón. 1997. Kinetic role of early intermediates in protein folding. *Curr. Opin. Struct. Biol.* 7:15–28.

Roder, H., and G. A. Elöve. 1994. Early stages of protein folding. *In* Mechanisms of Protein Folding: Frontiers in Molecular Biology. Oxford University Press, New York. 26–55.

Roder, H., G. A. Elöve, and S. W. Englander. 1988. Structural characterization of folding intermediates in cytochrome c by H-exchange labelling and proton NMR. *Nature.* 335:700–704.

Sauder, J. M., N. E. MacKenzie, and H. Roder. 1996. Kinetic mechanism of folding and unfolding of *Rhodobacter capsulatus* cytochrome c_2. *Biochemistry.* 35:16852–16862.

Sosnick, T. R., L. Mayne, and S. W. Englander. 1996. Molecular collapse: the rate-limiting step in two-state cytochrome c folding. *Proteins.* 24: 413–426.

Sosnick, T. R., L. Mayne, R. Hiller, and S. W. Englander. 1994. The barriers in protein folding. *Nature Struct. Biol.* 1:149–156.

Takahashi, S., Y.-c. Ching, J. Wang, and D. L. Rousseau. 1995. Microsecond generation of oxygen-bound cytochrome c oxidase by rapid solution mixing. *J. Biol. Chem.* 270:8405–8407.

Takahashi, S., S.-R. Yeh, T. K. Das, C.-K. Chan, D. S. Gottfried, and D. L. Rousseau. 1997. Folding of cytochrome *c* initiated by submillisecond mixing. *Nature Struct. Biol.* 4:44–50.

Tonomura, B., H. Nakatani, M. Ohnishi, J. Yamaguchi-Ito, and K. Hiromi. 1978. Test reactions for a stopped-flow apparatus. Reduction of 2,6-dichlorophenolindophenol and potassium ferricyanide by L-ascorbic acid. *Anal. Biochem.* 84:370–383.

Tsong, T. Y. 1976. Ferricytochrome c chain folding measured by the energy transfer of tryptophan 59 to the heme group. *Biochemistry.* 15:5467–5473.